arXiv:1304.3231v1 [cond-mat.stat-mech] 11 Apr 2013

Dynamic hysteretic features of the Ising-type thin films

Bahadır Ozan Aktaş
Dokuz Eylül University, Graduate School of Natural and Applied Sciences, TR-35160 Izmir, Turkey

Ümit Akıncı and Hamza Polat*
Department of Physics, Dokuz Eylül University, TR-35160 Izmir, Turkey

(Dated: April 12, 2013)

In order to elucidate the important characteristics of hysteretic response, such as types of the frequency dispersion curves, the decay of hysteresis loop area, the mechanism of domain nucleation and/or growth in the dynamic process, etc., a followup examination after the original work has been presented. The additive complementary treatment is essentially based on the results of recent preprint arXiv:1302.2727 concerning the effect of oscillatory perturbation on the surface enhancement phenomenon in magnetic thin films. Throughout the analysis, the best appropriate parameter values have been chosen since they would allow us to achieve striking results. The topology of the response for different layer indices in two regimes of modified surface exchange has been particularly emphasized.

PACS numbers: 64.60.Ht, 75.60.-d, 75.70.Kw, 75.70.-i
Keywords: Dynamic critical behavior, magnetic hysteresis, magnetic domains, thin film.

I. INTRODUCTION

Hysteresis is the signature of how the cooperative many-body system parameters respond dynamically to an alternating external magnetic field sweep. For the kinetic Ising-type systems, the most familiar one is originates as the ordinary magnetization (time-dependent magnetization) versus external field in the form of Lissajous curve. This ubiquitous phenomenon has been subject of intensive interest due to a broad range of applications. Hysteretic behavior is, however, a complicated process of a dynamic and nonlinear nature that elude serious treatment, both experimentally and theoretically since the area enclosed by the hysteresis loop (HL) is directly proportional to the energy loss in a magnetization-demagnetization cycle. The remanent magnetization (in other words residual magnetization which is the magnetization left behind in the system after an external magnetic field is removed) and coercive field which means that the intensity of the external magnetic field needed to change the sign of the magnetization has been calculated at several times in literature by benefiting from the hysteresis in order to understand and clarify the behavior of the system under consideration. HLs areal scaling law -which enables universality classification- has been manifested first by Steinmetz [1] empirically on his pioneering work dating back to the end of the nineteenth-century.

Many efforts have been devoted to prediction and experimental verification of the scaling behavior of the hysteresis loop area (HLA) for thin films (for a brief review of HLA scaling results see Ref. [2]). The recent series of studies about characteristics of the hysteretic response in thin films (the topic also constitutes the essence of our examination) have been also propounded by different researchers [3–6]. Low coercivity is desired in the core materials (or it is only used in recording for a short lifetime), which means low hysteresis loss per cycle of operation. Contrary to this, high coercivity is used in applications where magnetic recording media is frequently used or need to have a long life. This constant strategy is the main trend-setter in magnetic thin film design especially in recording applications [7]. In other respects, controlling thickness of film to obtain the magnetic hysteresis at a right shape to suit desired technological purpose has been the key issue in disguise [5]. Therefore, the core meaning of how the spontaneous spin formation mechanisms involved in these reduced structures are different form the bulk have become the focus of frequent investigation issues. However, to the best of our knowledge, there is not any systematic investigation regarding the hysteresis behavior and its influences on each layer of the ferromagnetic thin film due to the underlying complexity of the reduced dimension. So, there are some important issues which remain in suspense; frequency dispersion of HLA with corresponding remanence and coercivity for different layer indices in parallel with the classification of dispersion curves, topological evolution of the hysteretic response of each layer with respect to the modified surface exchange, etc.

Consequently, the aim of the study is to give a more complete picture of the overall hysteretic behavior of ferromagnetic thin films especially at different values of modified exchange interaction for a fixed temperature value (the temperature has been selected a certain criterion). For this purpose, we first investigate how the hysteretic properties of a film, including their relevant dispersion curves, depend on the dynamic system parameters by means of effective-field theory (EFT). After that we construct various kinds of hysteresis (in fact, they are collections of curves well-selected from the frequency dis-

* hamza.polat@deu.edu.tr

persion of the HLA) to confirm the results and to observe how the response depends on the layer index. Finally we give our results by discussing the magnetization reversal mechanism within reasonable bounds.

II. METHODOLOGY

From the theoretical point of view, one of the models more widely used to study the magnetic properties of surfaces is semi-infinite Ising model due to the crossover of dimensionality and their strong uniaxial anisotropy, so the system can be modeled by a layered Ising-type structure which consists of interacting L parallel layers. Each layer is defined as a regular lattice with coordination number $z = 4$. The familiar Hamiltonian of the thin film is given by,

$$\mathcal{H} = -\sum_{\langle ij \rangle} J_{ij} s_i s_j - h(t) \sum_i s_i \tag{1}$$

where s_i is the spin operator at a lattice site i and any spin variable can take the values $s_i = \pm 1$. As is known, $\langle \ldots \rangle$ subscript bracket symbolizes the nearest neighboring in first summation. The second summation is over all the lattice sites. The exchange interaction J_{ij} between the spins on the sites i and j takes the values according to the positions of the nearest neighbor spins. Two surfaces of the film have the intralayer coupling J_1. The interlayer coupling between the surface and its adjacent layer (i.e. layers 1, 2 and L, $L-1$) is denoted by J_2. For the rest of the layers, the interlayer and the intralayer couplings are assumed as J_3. The system has three exchange interactions where J_1, J_2, $J_3 > 0$ favors a ferromagnetic alignment of the adjacent sites as shown in Fig. (1) which has been presented in our prior work (see Ref. [8]) and the Zeeman term describes interaction of the spins with the field of the sinusoidal form

$$h(t) = h_0 \cos(\omega t), \tag{2}$$

where t is the time and h_0 is the amplitude of the oscillatory magnetic field with an angular frequency ω.

Our system is in contact with an isothermal heat bath at given temperature T. So, the dynamical evolution of the system may be given by non-equilibrium Glauber dynamics [9] based on a master equation. Number of L different representative magnetization time series for the system can be given by usual dynamical EFT equations which are obtained by differential operator technique [10, 11]. In order to handle the multi-spin correlations, a decoupling approximation (DA) [12] can be used as

$$\langle s_i^{(k)} \ldots s_j^{(k)} \ldots s_l^{(k)} \rangle = \langle s_1^{(k)} \rangle \ldots \langle s_j^{(k)} \rangle \ldots \langle s_l^{(k)} \rangle, \tag{3}$$

which is essentially identical to the Zernike approximation [13] in the bulk problem, and it has been successfully applied to a great number of magnetic systems including the surface problems [14–16]. Thus, the dynamical equations of motion for each layer are in the form of

$$\begin{aligned}
\tau \frac{dm_1}{dt} &= -m_1 + [A_1 + m_1 B_1]^z [A_2 + m_2 B_2], \\
\tau \frac{dm_2}{dt} &= -m_2 + [A_2 + m_1 B_2][A_3 + m_2 B_3]^z [A_3 + m_3 B_3], \\
&\vdots \quad \vdots \qquad\qquad \vdots \\
\tau \frac{dm_k}{dt} &= -m_k + [A_3 + m_{k-1} B_3][A_3 + m_k B_3]^z [A_3 + m_{k+1} B_3], \\
&\vdots \quad \vdots \qquad\qquad \vdots \\
\tau \frac{dm_{L-1}}{dt} &= -m_{L-1} + [A_3 + m_{L-2} B_3][A_3 + m_{L-1} B_3]^z [A_2 + m_L B_2], \\
\tau \frac{dm_L}{dt} &= -m_L + [A_2 + m_{L-1} B_2][A_1 + m_L B_1]^z.
\end{aligned} \tag{4}$$

Here m_k which is the magnetization time series of kth layer is defined as

$$m_k = \langle s_i^{(k)} \rangle, \quad k = 1, \ldots, L, \tag{5}$$

with the coefficients

$$\begin{aligned}
A_n &= \cosh(J_n \nabla) f(x)|_{x=0}, \\
B_n &= \sinh(J_n \nabla) f(x)|_{x=0},
\end{aligned} \tag{6}$$

where $n = 1, 2, 3$ and $\nabla = \partial/\partial x$ is one dimensional differential operator and the function $f(x)$ is given by

$$f(x) = \tanh[\beta(x + h(t))]. \tag{7}$$

Here $\beta = 1/k_B T$ and k_B represents the Boltzmann constant. The effect of the differential operator on an arbitrary function $f(x)$,

$$\exp(a\nabla) f(x)|_{x=0} = f(x + a)|_{x=0}, \tag{8}$$

with any real constant a.

By using the binomial expansion and writing the hyperbolic trigonometric functions in terms of the exponential functions we get the most compact form of Eq. (4) as

$$\begin{aligned}
\dot{m}_1 &= \frac{1}{\tau}\left(-m_1 + \sum_{\gamma=0}^{z}\sum_{\eta=0}^{1}\Lambda_1(\gamma,\eta)m_1^{\gamma}m_2^{\eta}\right),\\
\dot{m}_2 &= \frac{1}{\tau}\left(-m_2 + \sum_{\gamma=0}^{z}\sum_{\eta=0}^{1}\sum_{\nu=0}^{1}\Lambda_2(\gamma,\eta,\nu)m_2^{\gamma}m_1^{\eta}m_3^{\nu}\right),\\
&\vdots \quad \vdots \qquad\qquad \vdots\\
\dot{m}_k &= \frac{1}{\tau}\left(-m_k + \sum_{\gamma=0}^{z}\sum_{\eta=0}^{1}\sum_{\nu=0}^{1}\Lambda_3(\gamma,\eta,\nu)m_k^{\gamma}m_{k-1}^{\eta}m_{k+1}^{\nu}\right),\\
&\vdots \quad \vdots \qquad\qquad \vdots\\
\dot{m}_{L-1} &= \frac{1}{\tau}\left(-m_{L-1} + \sum_{\gamma=0}^{z}\sum_{\eta=0}^{1}\sum_{\nu=0}^{1}\Lambda_2(\gamma,\eta,\nu)m_L^{\gamma}m_{L-1}^{\eta}m_{L+1}^{\nu}\right),\\
\dot{m}_L &= \frac{1}{\tau}\left(-m_L + \sum_{\gamma=0}^{z}\sum_{\eta=0}^{1}\Lambda_1(\gamma,\eta)m_L^{\gamma}m_{L-1}^{\eta}\right).
\end{aligned} \tag{9}$$

where

$$\begin{aligned}
\Lambda_1(\gamma,\eta) &= \binom{z}{\gamma}\binom{1}{\eta}A_1^{z-\gamma}A_2^{1-\eta}B_1^{\gamma}B_2^{\eta},\\
\Lambda_2(\gamma,\eta,\nu) &= \binom{z}{\gamma}\binom{1}{\eta}\binom{1}{\nu}A_2^{1-\eta}A_3^{z+1-\gamma-\nu}B_2^{\eta}B_3^{\gamma+\nu},\\
\Lambda_3(\gamma,\eta,\nu) &= \binom{z}{\gamma}\binom{1}{\eta}\binom{1}{\nu}A_3^{z+2-\gamma-\eta-\nu}B_3^{\gamma+\eta+\nu}.
\end{aligned} \tag{10}$$

Here, $1/\tau$ is the transition per unit time in a Glauber type stochastic process and throughout our calculations it is selected as $\tau = 1$ for simplicity. Self-consistent nonlinear ordinary differential equations in Eq. (9) are solved by fourth order Runge-Kutta method (RK4) to get the evolution of the $m_k(t)$ by regarding the equation as an initial value problem.

The system has three dependent Hamiltonian variables, namely frequency of external magnetic field ω, amplitude h_0 and the film thickness L. For certain values of these parameters, temperature and the J_1, J_2, J_3 interaction constants, RK4 will give convergency behavior after some iterations i.e. the solutions have property $m(t) = m(t + 2\pi/\omega)$ for arbitrary initial value for the magnetization ($m(t = 0)$). Each iteration, i.e. the calculation of magnetization at $t + 1$ from previous magnetization for t, is now performed for these purpose whereby the RK4 iterative equation is being utilized to determine the magnetization for every i. In order to keep the iteration procedure stable in our simulations, we have chosen 10^4 points for each RK4 step. Thus, after obtaining the convergent region and some transient steps (which depends on Hamiltonian parameters and the temperature) the layers' average magnetization can be calculated from

$$Q_k = \frac{\omega}{2\pi}\oint m_k(t)dt \tag{11}$$

where m_k is a stable and periodic function and finally the dynamical order parameter (DOP) can be calculated by the arithmetic mean as

$$Q = \frac{1}{L}\sum_{k=1}^{L} Q_k. \tag{12}$$

As cut-off condition for numerical self-consistency, we defined a tolerance

$$\left|Q_k|_{t-2\pi/\omega}^{t} - Q_k|_{t}^{t+2\pi/\omega}\right| < 10^{-5}, \tag{13}$$

meaning that the maximum error as difference between the each consecutive iteration should be lower than 10^{-5} for all step. On the other hand the HLA corresponding to energy loss due to the hysteresis is defined as

$$A^{(k)} = -\oint m_k(t)dh(t) = h_0\omega\oint m_k(t)\sin(\omega t), \tag{14}$$

and the modified surface exchange interaction has been defined to determine the different characteristic behavior of the system in certain range as

$$J_1 = J_3(1 + \Delta_s). \tag{15}$$

There are three possible states for the system, namely F, P and the coexistence phase (F+P). The total magnetization time-series $m(t)$ in convergent region is satisfied by this condition

$$m(t) = -m(t + \pi/\omega) \tag{16}$$

in the P phase which is called the symmetric solution. On the other hand, in the F phase, the solution does not satisfy Eq. (16) and this solution is called as non-symmetric solution which oscillates around a non-zero magnetization value, and does not follow the external magnetic field i.e. the value of Q is different from zero. In these two cases, the observed behavior of magnetization is regardless of the choice of initial value of magnetization $m(0)$ whereas the last phase has magnetization solutions symmetric or non-symmetric depending on the choice of the initial value of magnetization corresponding to the coexistence region where F and P phases overlap. The main goal of the treatment is adjunctly manifesting the frequency dispersion of the HLA and corresponding coercivity ($H_c^{(k)}$) with remanence ($M_r^{(k)}$) of layers. Note that, more details about formulation and the reasons for selection procedure of the related values of system parameters at which the calculations carried out can be seen in Ref. [8].

III. RESULTS AND DISCUSSION

With the guidance of the work presented by Aktaş et al. [8], the frequency dispersion of the HLA and the corresponding coercivity with remanent magnetization for a pure crystalline ferromagnetic thin film with thickness $L = 7$ are globally presented in Figs. (1), (2) and (3). As a result of evaluations by the conviction that we have reached, the dependency characteristics with varying frequency has an intersection at a critical value of the modified exchange interaction. For instance, Fig. (1) shows the hierarchical reversal of the HLA in each layer as changing Δ_s. At a fixed h_0, it can be seen that the surface has the lowest loop area in $\Delta_s < \Delta_s^*$ till the symmetry loss occurs as well as the innermost layer has the lowest loop area in the opposite regime (namely $\Delta_s > \Delta_s^*$). In other respects, the layer indices are of no importance in frequency dependency at the critical value of modified exchange interaction, i.e. if the modified exchange interaction ever had it's critical value all the layers would have the same hysteretic behavior. Areal magnitude sequence of hysteresis loop for the layers becomes reversed between each other at Δ_s^*. Physical mechanism mentioned above can be briefly explained as follows: At a fixed h_0 and Δ_s value in $\Delta_s < \Delta_s^*$ regime but on increasing layer index k (e.g. $k = 1$ corresponds to the surface layer) hysteresis loop becomes larger at low ω but it slightly gets smaller at high ω. This is since for inner layers there are relatively more neighboring per magnetic-sites which cause locally larger magnetic interaction. With a stronger magnetic interaction in that local lattice region, it becomes more difficult for spins to follow the field and the hysteresis almost tends to be asymmetric. Surface atoms are embedded in an environment of lower symmetry than that of the inner atoms and consequently the exchange constants between atoms in the surface region may differ from the bulk one for experimental evidence. The lower Δ_s regime corresponds to surface type of magnetic ordering with this aspect. However, one can reverse the whole aforementioned scenario by controlling (actually by increasing) Δ_s, i.e. in $\Delta_s > \Delta_s^*$ regime increasing layer index k hysteresis loop becomes smaller at low ω but slightly larger at high ω. This is since for inner layers there are relatively more neighboring but far less exchange constants per magnetic-sites which cause relatively smaller magnetic interaction than that of the surface one anymore. Finally, theoretical evidence forced us to remark that the free surface couldn't break the translational symmetry since the hysteretic and/or magnetic properties of the free surfaces seriously overlap with the bulk one at the critical value of Δ_s (namely Δ_s^*). The investigations depicted in Figs. (2) and (3) are also consistent with the whole arguments about the mechanism.

At a fixed h_0 and Δ_s, for purely symmetric region, with increasing ω, A_k increases at low ω whereas it decreases as ω whereas it decreases in agreement with the well-known behavior in literature where frequency at the peak ω_c corresponds to the phase-lag. In $\Delta_s < \Delta_s^*$ regime, this ω_c shifts to lower values of ω as increasing the layer index k due to the locally stronger magnetic interaction. With the same reason, at a fixed ω, A_k increases (especially at low ω) with increasing layer index k for $\Delta_s < \Delta_s^*$ while reverse of the overall arguments given above are valid for $\Delta_s > \Delta_s^*$ regime. One can easily observe the intersection on ω_c values of layers via changing Δ_s parameter.

In addition, in Fig. (1) and both Fig. (2) with (3), the coercivity $H_c^{(k)}$ increases with increasing the field amplitude h_0 whereas increasing in remanence $M_r^{(k)}$ can be seen in significantly asymmetric region. It means that HLA A_k increases with increasing h_0 and this increment is dependent of the other system parameters. This is since the higher amplitude provides higher magnetic energy to the system and this higher energy provides more magnetic force in causing the spins to follow the field. Consequently, the frequency at the peak (ω_c) in symmetric region for a selected layer index and value of Δ_s shifts to higher ω as the phase-lag between ordinary magnetization and field signal is smaller for the higher amplitude.

Next, the hysteresis loop collection of each layer for related system parameters and selected the best three appropriate values of frequency are presented in Fig. (4). As is acquainted with the low frequency limit, the magnetization can be more saturated and this shows itself as the dominant magnetization processes in the different regions of the curve (i.e. reversible boundary displacements, irreversible boundary displacements and magnetization rotation). The figure shows that the hysteretic response of each layer clearly has the same characteristics at the critical value of the modified exchange Δ_s^*

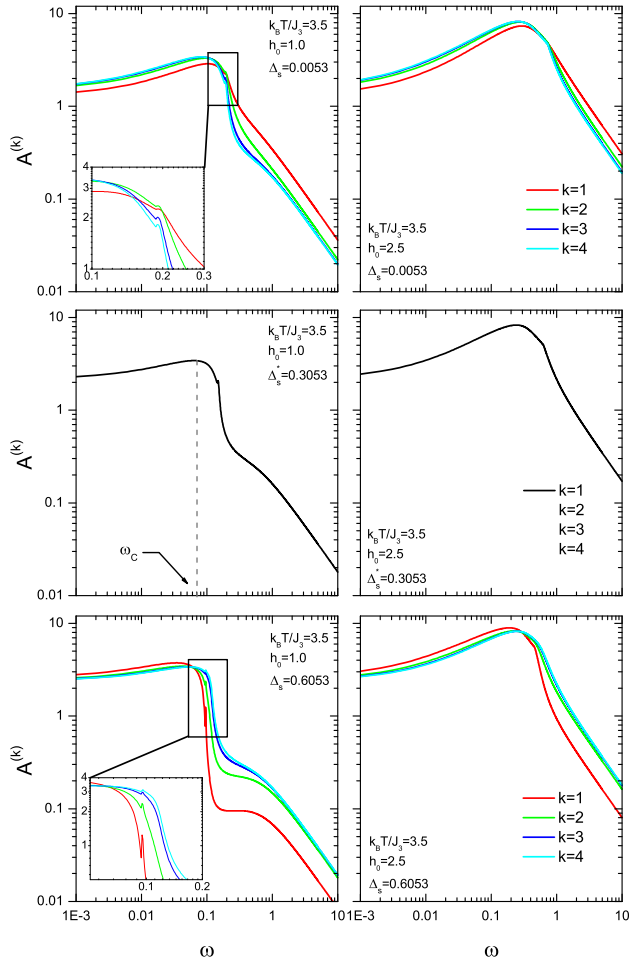

FIG. 1. (Color online) The frequency dispersion of HLA for each layer of the film with thickness $L = 7$ at a fixed temperature $k_BT/J_3 = 3.5$. The curves as seen in each group of triple-column have been plotted for the selected amplitude representatives as $h_0 = 1.0$ and 2.5. They profiles across the film differ qualitatively in two regimes ($\Delta_s < \Delta_s^*$ and $\Delta_s > \Delta_s^*$). Each inset is stated in terms of visual clarity.

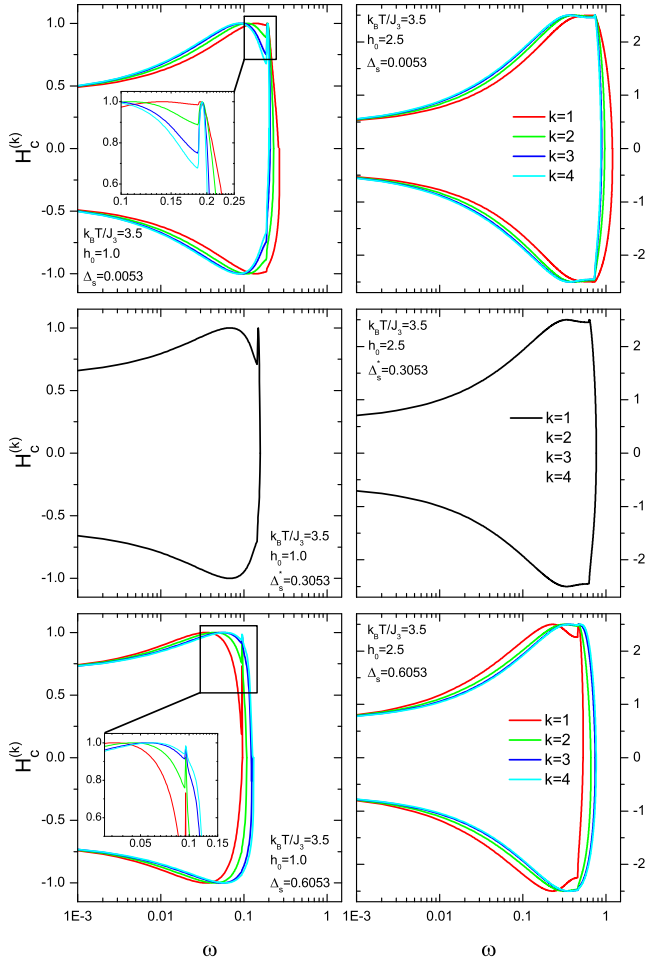

FIG. 2. (Color online) The frequency dispersion of coercive field for the same selected system parameters of the film with thickness $L = 7$ depicted in Fig. (1). Each inset is stated in terms of visual clarity.

independently with the other parameters. Hierarchical reversal of the hysteresis loop of each layer for various values of amplitudes and/or frequency also can be seen in Fig. (4) by following the group of three columns including the related regimes of Δ_s ($\Delta_s < \Delta_s^*$, $\Delta_s \equiv \Delta_s^*$ and $\Delta_s > \Delta_s^*$). One can observe the effects of symmetry on this reversal mechanism (following ability of the layers to external field sweep) by comparing the representative amplitudes between each other. At the fixed $\Delta_s \equiv \Delta_s^*$ value, for $h_0 = 2.5$ representative, it can be seen that the hysteresis loop has a saturated s-shape and tends to increase in size with increasing ω at low frequency region e.g. $\omega < 0.3$. However, on further increasing ω, the loop gets its maximum area and later reduces to an oval shape with its major axis parallel to the field axis. This is the result of phase-lag between the ordinary magnetization and the field signal. At very low ω, the field period is large and the magnetic spins have sufficient time to follow the field signal so the phase-lag between the ordinary magnetization and field signal is small. The system is strong enough to follow the external perturbation at those limitations, hence the hysteresis loop looks like a slim s-shape. However, on increasing ω, the field sweeps faster and the spins have less time in following the field. Consequently, the phase-lag gets larger and so does the hysteresis. At a particular point, when the phase-lag approaching its critical value, the hysteresis gets its maximum size. After that, if ω still increases in small doses, the spins feel very difficult in following the field so the overall magnetization does not change much as the field changes. Therefore the hysteresis turns its shape in oval-shape with its major axis lying along the field axis. Additionally, for $h_0 = 1.0$ representative, a rare pre-symmetry loss morphology can be seen by following the topological evolution of hysteresis loop with increasing frequency at the fixed $\Delta_s > \Delta_s^*$. For instance, as seen at $\omega = 0.07$ value, an exotic left-handed s-shape beyond

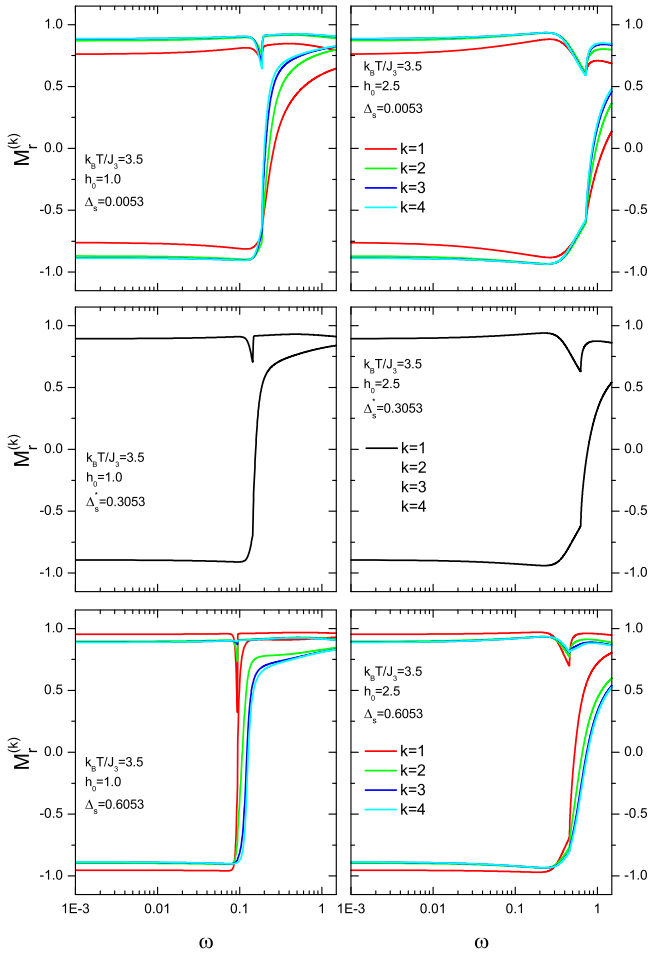

FIG. 3. (Color online) The frequency dispersion of remanent magnetization for the same selected system parameters of the film with thickness $L = 7$ depicted in Fig. (1).

the oval form temporally takes place between maximal area frequency ω_c and the frequency value of symmetry loss which is absolutely stated about $\omega > \omega_c$. The result of general assessment about the hysteresis collection as follows: For low frequencies, the hysteresis loop is in the form of saturated s-shape and tends to increase in size with increasing ω at low frequency region. At a critical ω_c value, the loop gets its maximum area. On further increasing ω, hysteresis enters into the process of smooth directional-veering and it has a left-handed s-shape until the symmetry loss. Forthwith, the symmetry loss occurs at a characteristic frequency value and after that point, the hysteresis has an asymmetric shape.

The process stated between at the beginning of directional-veering and symmetry loss deserves a scrutiny. As seen in Figs. (1), (2) and (3), symmetry loss takes place at a gibbous-like eminentia. This phenomenon has been zoomed in Figs. (1) and (2) for better visibility. Particularly, as seen in Fig. (3), both of the positive and negative remanence appears at low frequencies, but only positive values survive at high frequencies due to the symmetry loss. The related eminentia shows itself more specifically on right arm of the mutual coercivity and it is far more distinct in surfaces for low amplitudes in condition with $\Delta_s > \Delta_s^*$. Notice that the encountered symmetry loss characteristics for all observations on this problem are the member of Type II.b family of frequency dispersion presented by Aktaş et al. [17]. Low amplitude relatively provides smaller magnetic energy to the system and this weak energy could not provide enough magnetic force in causing the spins to follow the field. This means the surfaces fall all over itself to adopt to the asymmetric phase in the $\Delta_s > \Delta_s^*$ regime, so, the surfaces have extremely left-handed saturated s-shape hysteretic response within that period. It is also of interest to consider the topological evolution of the hysteresis as changing ω to investigate how it relates with spin formation (namely magnetic domains) growth and/or nucleation mechanism. Two branches of the hysteresis curve intersect each other at ω_c and the HLA has the global maxima related to the multiplying of its two-axis. Therefore, the magnetic moment remains approximately constant value in the half-time period of external field. At the fixed values of $\omega < \omega_c$ and $\omega > \omega_c$ respectively, corresponding hysteresis curves are topologically contra-oriented mutually and completely different growth mechanism is onset. According to times-series of the magnetization versus the external magnetic field, increasing the field frequency at first, obstructs the saturation of the ordinary magnetization due to the decreasing energy coming from the oscillating magnetic field in a half-time period which facilitates the late stage domain growth by tending to align the moments in its direction (i.e. the magnetization begins to fail following the oscillatory field) and this makes the occurrence of the frequency increasing route to continuous dynamical phase transition due to the incomplete reversal of magnetic moments. The aforementioned directional-veering mechanism in the $\Delta_s < \Delta_s^*$ regime begins to lose its significance. Since as the Δ_s is lowered more and more then the dipole-dipole interaction-induced energy contribution gets smaller. The quantity of the energy contribution which comes from the dipole-dipole interaction corresponds to the self-volition to remain in the dynamically symmetric phase of the system. Hence, the surfaces can stay in the symmetric phase in the smaller frequency until the frequency of the external field becomes greater than the relaxation time of the system.

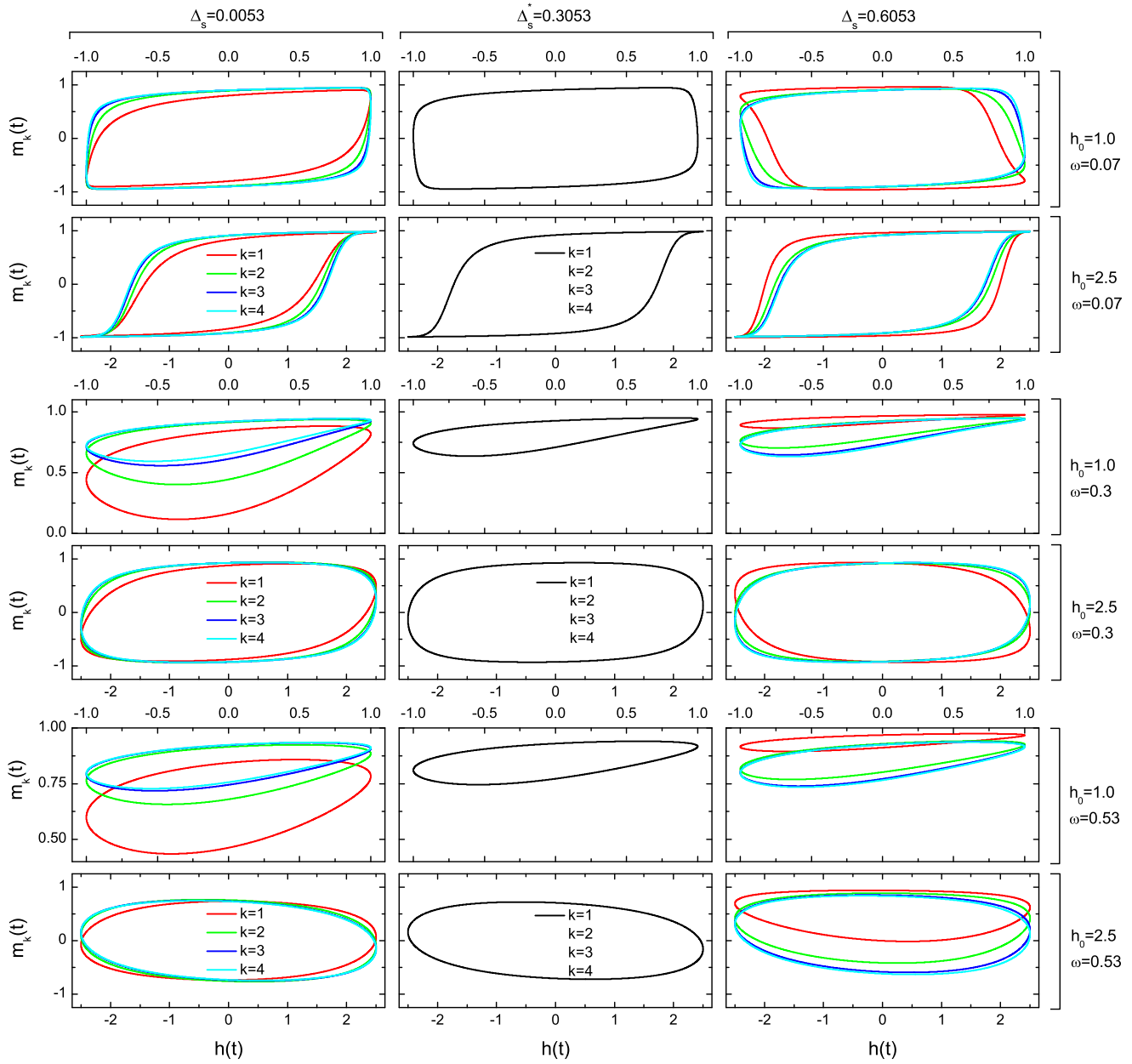

FIG. 4. (Color online) The related HL collection of each layer for the film with thickness $L = 7$. Modified exchange interaction Δ_s ranges from 0.0053 (first column) to 0.3053 (second column) and 0.6053 (third column) with varying frequency as $\omega = 0.07$, 0.3 and 0.53 for related amplitude representatives at $k_BT/J_3 = 3.5$.

IV. CONCLUSION

As a complementary work, the effect of Δ_s on the topological evolution and strength of HLA for each layer has been discussed by means of effective field theory based on a standard decoupling approximation for dynamical Ising-type thin films of $L = 7$ driven by an external oscillatory magnetic field with inner coordination number $z = 4$. The time evolution of the system has been presented by utilizing a Glauber type stochastic process. For pre-selected values of the system parameters, our investigation has been focused on frequency dispersion of HLA, coercivity and the remanence of each layer.

Concretely speaking, in order to propound a link between domain growth and/or nucleation mechanism and symmetry loss in magnetic thin films, we appeal to hysteresis for its topological evolution in respect to the frequency for throughout our work. Hence, some unpretentious improvements on the relation has been developed in accordance with the explanations given before in literature by some experts.

In conclusion, we hope that the results obtained in this

work would shed light on the further investigations of the dynamic nature of the critical phenomena in pure crystalline ferromagnetic thin films and would be beneficial from both theoretical and experimental points of view.

ACKNOWLEDGEMENTS

The numerical calculations reported in this paper were performed at TÜBİTAK ULAKBİM (Turkish agency), High Performance and Grid Computing Center (TRUBA Resources) and this study has been completed at Dokuz Eylül University, Graduate School of Natural and Applied Sciences. One of the authors (B.O.A.) would like to thank the Turkish Educational Foundation (TEV) for full scholarship.

[1] C. P. Steinmetz, Trans. Am. Inst. Electr. Eng. **9**, 3 (1892).
[2] J. S. Suen and J. L. Erskine, Phys. Rev. Lett. **78**, 3567 (1997).
[3] Q. Jiang, H. N. Yang, and G. C. Wang, Phys. Rev. B **52**, 14911 (1995).
[4] Y. L. He and G. C. Wang, Phys. Rev. Lett. **70**, 2336 (1993).
[5] J. S. Suen, M. H. Lee, G. Teeter and J. L. Erskine, Phys. Rev. B **59**, 4249 (1999).
[6] Y. Laosiritaworn, Thin Solid Films **517**, 5189 (2009).
[7] T. Osaka, T. Asahi, J. Kawaii, and T. Yokoshima, Electrochim. Acta **50**, 4576 (2005).
[8] B. O. Aktaş, Ü. Akıncı, and H. Polat, arXiv:1302.2727.
[9] R. J. Glauber, J. Math. Phys. **4**, 294 (1963).,
[10] R. Honmura and T. Kaneyoshi, J. Phys. C: Solid State Physics **12**, 3979 (1979).
[11] T. Kaneyoshi, Acta Phys. Pol. A **83**, 703 (1993).
[12] J. W. Tucker, J. Magn. Magn. Mater. **102**, 144 (1991).
[13] F. Zernike, Physica A **7**, 565 (1940).
[14] T. Balcerzak, J. Magn. Magn. Mater. **97**, 152 (1991).
[15] T. Kaneyoshi, R. Honmura, I. Tamura, and E. F. Sarmento, Phys. Rev. B **29**, 5121 (1984).
[16] T. Kaneyoshi, I. Tamura, and E. F. Sarmento, Phys. Rev. B **28**, 6491 (1983).
[17] B. O. Aktaş, Ü. Akıncı, and H. Polat, Physica B **407**, 4721 (2012).